Journal of Biomaterials and Nanobiotechnology, 2019, 10, 196-211
http://www.scirp.org/journal/jbnb
ISSN Online: 2158-7043
ISSN Print: 2158-7027

Characterization of BellaGel SmoothFine® Implant Surfaces and Correlation with Capsular Contracture

Sun-Young Nam[1*], Miji Lee[1*], Byung Ho Shin[1], Bassem Elfeky[1], Yang U. Lee[1], Dae Hee Moon[2], Daeun Seo[2], Chan Yeong Heo[1#]

[1]Department of Plastic & Reconstructive Surgery, Seoul National University Bundang Hospital, Seongnam, Republic of Korea
[2]HansBiomed Corp., Daejeon, Republic of Korea
Email: #lionheo@gmail.com

How to cite this paper: Nam, S.-Y., Lee, M., Shin, B.H., Elfeky, B., Lee, Y.U., Moon, D.H., Seo, D. and Heo, C.Y. (2019) Characterization of BellaGel SmoothFine® Implant Surfaces and Correlation with Capsular Contracture. *Journal of Biomaterials and Nanobiotechnology*, **10**, 196-211.
https://doi.org/10.4236/jbnb.2019.104012

Received: September 22, 2019
Accepted: October 25, 2019
Published: October 28, 2019

Abstract

BellaGel SmoothFine® implant is a novel nanotextured silicone breast implant. The objective of this study was to characterize differences of BellaGel SmoothFine® surfaces with commercial available implant surfaces in terms of texture, topography, and wettability as well as the behavior of capsular contracture. The surface textures of breast implants from two different manufacturers (Hans Biomed and Motiva) were evaluated. The implants utilized in this study were BellaGel Smooth®, BellaGel Textured®, BellaGel SmoothFine® or Motiva SilkSurface®. The shell textures of these implants were characterized using a scanning electron microscopy, three dimensional confocal laser scanning microscope, and contact angle goniometer. Silicone breast implants were emplaced beneath the panniculus carnosus muscle on the dorsum of Sprague Dawley rats and observed for up to 8 weeks postoperative days. The fibrous capsules around silicone implants were explanted for histological examination. BellaGel SmoothFine® exhibits a relatively flat, with little or no depth in the texturing, 5.96 ± 0.41 μm surface roughness, and a contact angle of 103.14 ± 2.06 BellGel SmoothFine® implant resulted in significant decreases in capsule thickness ($P < 0.05$) and collagen production ($P < 0.05$) at 8 weeks with respect to the BellaGel Smooth® and BellaGel Textured® implant groups. Significant ($P < 0.05$) decreases in inducible nitric oxide synthase, an inflammation marker, were observed in the BellGel SmoothFine®. Fibrous tissue formation markers (Vimentin and alpha-smooth muscle actin) were significantly reduced in BellaGel SmoothFine® surfaces versus BellaGel Smooth® surfaces ($P < 0.05$) or BellaGel Textured® groups ($P < 0.05$). Overall, these findings suggest that the nanotextured BellaGel SmoothFine® implant is associated with less breast implant derived capsular contracture than other surfaces.

*Sun-Young Nam and Miji Lee contributed equally to this work.

Keywords

Silicone Breast Implant, Capsular Contracture, Topography, Roughness, iNOS

1. Introduction

According to a 2013 report from the American Society of Plastic Surgeons, there are more than 200,000 women in the USA who had reconstructive or cosmetic breast augmentations. The medical literature describes that silicone gel-filled breast implants are linked with significant adverse health effects [1] [2]. The most common local complication associated with silicone gel-filled breast implant is capsular contracture, with a combined overall incidence of 10.6% [3] [4] [5] [6]. Capsular contracture is a multifactorial fibrotic foreign body reaction that promotes the hardening and tightening of the capsule at the contact site between the tissue and implant, which then causes dissatisfaction and pain after breast augmentation in addition to deformity and device failure [7]. Though the pathogenesis of capsular contracture has not been fully elucidated, a variety of causal associations including surface texture of the breast implant have been proposed to date [8].

The surface texture of the shell surrounding breast implant acts as the interface between the breast tissue and device [9] and its understanding is important in the field of implantation. They can markedly alter the pathophysiology and directly influence cellular biology, body tissues, and fibrous capsule development, specially the adherence of the tissue to the breast implant and the alignment of collagen fibers [8] [10] [11]. Traditionally, there are two main kinds of implants: smooth and textured implants. Smooth-surface implants are used worldwide; however, the prevalence of capsular contracture is higher with the smooth implants than others. Meta-analyses studies showed approximately 5 times increase in the contracture rate on smooth surface with respect to textured surfaces [12] [13]. Textured-surface implants, which can disrupt the contractile forces, were developed to minimize capsular contracture [8]. However, serious complications such as double capsule formation, late seroma, and anaplastic large cell lymphoma (ALCL) have been appeared for textured implants due to their aggressive texturization [14] [15].

Recently, numerous articles have proposed the use of nanometric surface topographies to induce specific cellular behavior like cell proliferation, attachment, migration, and differentiation, which affect the prevalence rate of capsular contracture [8] [16] [17] [18] [19] [20]. Surfaces with nanoscale roughness closer to cellular dimensions are known to exhibit profound effects on cells and also produce a reduced foreign body response [21] [22]. BellaGel SmoothFine® implants have a novel nano textured surfaces. The complication rates of BellaGel SmoothFine® were almost 10 times less than any other devices

in our practice [23]. Our intuitive aim here is to evaluate the tissue's reaction to the BellaGel SmoothFine® surface texture with different surfaces using a rat implant model.

2. Materials and Methods

2.1. Breast Implants

Each shell of implants was obtained from 4 different breast implant devices (Table 1).

2.2. Scanning Electron Microscope (SEM)

A 2-cm^2 shell sample was obtained from each of BellaGel Smooth®, BellaGel Textured®, BellaGel SmoothFine®, and Motiva SilkSurface® implants. These specimens were cleaned twice in isopropylalcohol and viewed via an SEM (Hitachi, Tokyo, Japan). Analysis was done at accelerating voltage of 5 keV. The electron beam intensity was I = 10 - 11 A.

2.3. 3D Confocal Images

Physical properties of silicone breast implant surfaces including roughness, skewness, and kurtosis were observed by looking at their topographical features using a 3D confocal laser scanning microscope (LEXT OLS5000, Olympus Corporation, Tokyo, Japan). The experiments have been performed on 3 sample areas.

2.4. Wettability

Wettability assessment was carried out using a contact angle meter Phoenix-MT(T) (SEO, Suwon, Gyeonggido, Korea). The experiments were undertaken three times to ensure significance of the tests.

2.5. *In Vivo* Animal Experiment

Sixty Sprague-Dawley rats with a body weight of about 250 - 300 g (Orientbio, Seongnam, Gyeonggido, Korea) were maintained in an exceedingly 12/12 light/dark cycle under a pathogen-free condition and given water ad libitum. Animal care and experimental procedures were approved from the Institutional Animal Care and Use Committee of Seoul National University Bundang Hospital

Table 1. Breast implant types included in this study.

Designation	Trade Name	Manufacturer	Surface Manufacturing Method
Smooth	BellaGel Smooth®	HansBiomed	None
Macro	BellaGel Textured®	HansBiomed	Salt loss
Smooth	BellaGel SmoothFine®	HansBiomed	Imprinting
Smooth	Motiva SilkSurface®	Motiva	Imprinting

(approval number: N-1803/454-602).

In this study, 5 rats were allocated to each group and divided into four groups: 1) BellaGel Smooth® implant, 2) BellaGel Textured® implant, 3) BellaGel SmoothFine® implant, and 4) Motiva SilkSurface® implant. Each animal was anesthesed through inhalation using isoflurane (Hana Pharm, Seoul, Korea) and the incision site was made approximately 2 cm long on the dorsal part of rat. Subsequently, silicone breast implants were placed to the subpaniculus pocket. After 1, 2, and 8 weeks with the implant, rats were sacrificed with carbon dioxide.

2.6. Hematoxylin & Eosin Staining

Implants were excised in block with the surrounding tissue. Harvested specimens were fixed with 10% neutral buffered formalin and embedded in paraffin. Sections (5 μm) of tissue samples were stained with hematoxylin and eosin (H & E) before dewaxing and dehydration for histological analysis. Each stained slide was examined at × 100 magnification using a microscope (Carl Zeiss, Germany). The capsular thickness was calculated using Image J software (National Institutes of Health, Bethesda, MD, USA).

2.7. Masson's Trichrome Staining

Masson's Trichrome stain was performed according to manufacturer's instructions (Polysciences, Pennsylvania, USA).

2.8. Western Blot Analysis

The capsule tissue around silicone breast implant was prepared using a RIPA buffer (Sigma Aldrich, MO, USA) that contained phosphatase inhibitor cocktail (BioPrince, Chuncheon, Gangwon, Korea). Samples were then denatured by heating for five min and immediately placed on ice. After centrifugation, aliquots containing approximately 60 μg protein were separated by gel electrophoresis. After electrophoresis, the protein was transferred from the gel onto nitrocellulose membranes and then the membranes were blocked in 5% skim milk for 2 h. After blocking, the membranes were subjected to western blotting with antibodies for iNOS, α-SMA, ARG1 (1:1000; Abcam, Cambridge, UK), Vimentin and β-actin (1:1000; Santa cruz, CA, USA) at 4˚C for overnight. The blot was incubated with secondary antibodies (1:5000 in TBST, rabbit for iNOS and α-SMA; mouse for ARG1 and β-actin) for 1 h for protein detection. Finally, proteins were detected using the enhanced chemiluminescence reagent (Amersham Co. Newark, NJ, USA) following the manufacturer's instruction. The density of protein bands was measured using the Image J (National Institutes of Health, USA). The relative quantities were normalized by β-actin.

2.9. Statistical Analysis

All values are reported as means ± S.E.M. (standard error of the mean). Statistic-

al analyses were performed using SPSS statistical software (SPSS 11.5, Armonk, NY, USA). For all data, significant differences were determined using an unpaired *t*-test. For all analyses, $P < 0.05$ was defined as statistically significant.

3. Results

3.1. Texturing Analysis of BellaGel SmoothFine® Implant

BellaGel Smooth® texture was found a characteristic relatively flat appearance, with no height or no depth in the texturing and occasional surface irregularity (Figure 1). The BellaGel Textured® has striking surface characteristics and is made up of the pitted irregular cuboid appearance of the pores ("open-cell network") with sizes ranging from 100 to 400 μm width and depths varying between

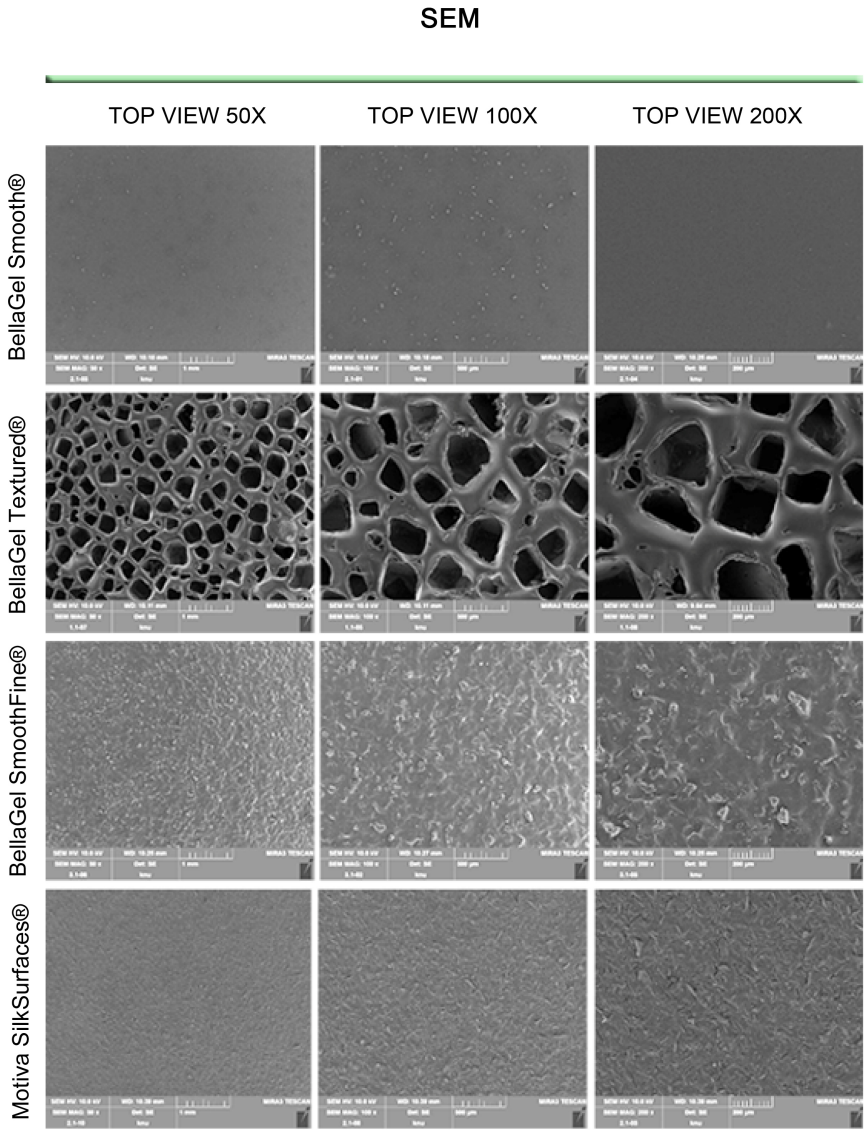

Figure 1. Texturing analysis of BellaGel SmoothFine® implant. SEM images of the top view (50×, 100×, and 200×) of BellaGel Smooth®, BellaGel Textured®, BellaGel SmoothFine®, and Motiva SilkSurfaces®.

100 and 400 μm. It has an average well density of six per mm^2 and pores composed of 80% of the total surface area (pores with 70 nm diameter). BellaGel SmoothFine® and Motiva SilkSurface® has more physically similar shapes and a more random and bumpy surface topography (Figure 1).

3.2. Surface Characterization of BellaGel SmoothFine® Implant

The surface area per mm^2 from 4 breast implant devices ranged from 1.0 mm^2 for the BellaGel Smooth® to 4.62 mm^2 for the BellaGel Textured® (Table 2). The BellaGel SmoothFine® and Motiva SilkSurface® have the surface area value, with 1.29 ± 0.01 mm^2 and 1.32 ± 0.02 mm^2, respectively.

Surface roughness is defined as the variance in the surface height with respect to the reference plane. Of the four implant textures tested, the BellaGel Smooth® surface contains a nano-scale roughness value of 0.40 μm ± 0.20 μm (Table 2 and Figure 2). The relatively large increased peak roughness value obtained for

Table 2. 3D surface parameters including surface area, roughness, kurtosis, and skewness.

Breast implant	Surface area	Roughness	Kurtosis	Skewness
BellaGel Smooth®	1.00 ± 0.00	0.40 ± 0.20	14.70 ± 12.56	0.45 ± 0.53
BellaGel Textured®	4.62 ± 1.25	100.10 ± 10.40	1.90 ± 0.14	−0.65 ± 0.19
BellaGel SmoothFine®	1.29 ± 0.01	5.96 ± 0.41	4.23 ± 0.68	0.36 ± 0.19
Motiva SilkSurface®	1.32 ± 0.02	3.05 ± 0.82	5.03 ± 1.26	0.89 ± 0.33

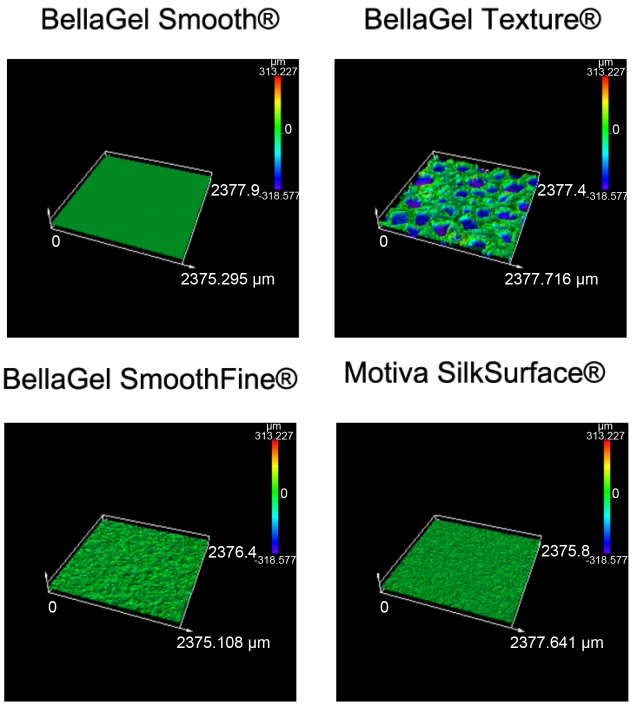

Figure 2. Surface characterization of BellaGel SmoothFine® implant. Confocal laser 3-D topography of BellaGel Smooth®, BellaGel Textured®, BellaGel SmoothFine®, and Motiva Silk-Surfaces®.

the BellaGel Textured® surfaces (100.10 μm ± 10.40 μm), which were about 250 times rougher than the BellaGel Smooth® surfaces (Table 2 and Figure 2). The BellaGel SmoothFine® surface has a roughness value of 5.96 μm ± 0.41 μm, which is relatively less rough than the BellaGel Textured® surface ($P < 0.001$). Motiva SilkSurface® contains nano-scale features with an average roughness of 3.05 μm ± 0.82 μm, this low roughness therefore would reduce the friction and particle lose (Table 2 and Figure 2).

The positive skewness values ($Sk > 0$) exhibited by the BellaGel Smooth® (Sk = 0.45 ± 0.53), BellaGel SmoothFine® (Sk = 0.36 ± 0.19), and Motiva SilkSurface® (Sk = 0.89 ± 0.33) implants suggests more peaks than valleys on the surfaces of these samples (Table 2). In contrast, the negative skewness value ($Sk < 0$) exhibited by the BellaGel Textured® (Sk = −0.65 ± 0.19) indicates the presence of more valleys than peaks on the surfaces (Table 2).

The BellaGel Smooth® surfaces exhibited an excess kurtosis value (Sku = 14.70 ± 12.56) suggesting that a repetitive surface with spikes. The smaller kurtosis values obtained for the BellaGel Textured® (1.90 ± 0.14), BellaGel SmoothFine® (4.23 ± 0.68), and Motiva SilkSurface® (5.03 ± 1.26) implants suggesting that bumpier and random surface.

Contact angle measurement was carried out to investigate the hydrophobicity of the surface texture. All implants were hydrophobic with contact angles all greater than 100˚ (Figure 3). From the measurements it was determined that the BellaGel Smooth® and BellaGel SmoothFine® surface were less hydrophobic than others, exhibiting a lower contact angle of 102.76˚ ± 0.62˚ and 103.14˚ ± 2.06˚, respectively (Figure 3) while the larger contact angle of 125.11˚ ± 2.35˚ and 121.61˚ ± 5.54˚ were obtained for the Motiva SilkSurface® and the BellaGel Textured® surface, respectively (Figure 3). The values indicate that the BellaGel Textured® surface and Motiva SilkSurface® and is less wettable than the BellaGel Smooth® and BellaGel SmoothFine® surface (Figure 3).

3.3. Effect of BellaGel SmoothFine® Implant on Capsule Formation

We compared the fibrous capsule development with respect to the implant surface texture of each implant device based on the contact site of the implant. The capsules wall diameter around the BellaGel Smooth® and BellaGel Textured®

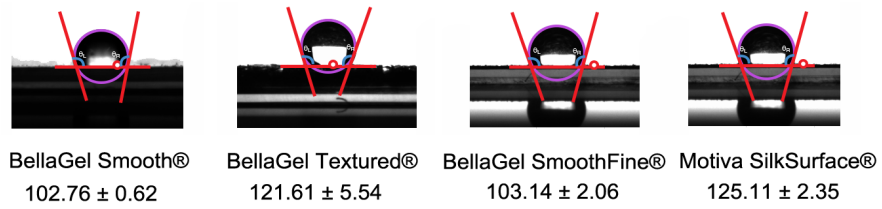

Figure 3. Contact angle analysis of BellaGel SmoothFine® implant. The assessment of contact angle of BellaGel Smooth®, BellaGel Textured®, BellaGel SmoothFine®, and Motiva SilkSurfaces® was carried out using a contact angle meter Phoenix-MT(T) (SEO, Suwon, Gyeonggido, Korea). The experiments were undertaken three times to ensure significance of the tests.

surface appeared significantly thicker than those around the BellaGel SmoothFine® and Motiva SilkSurface®. The average capsular thickness was 964.03 ± 20.05 μm in the BellaGel Smooth group®, compared with 935.9 ± 51.4 μm in the BellaGel Textured® group. This difference was not statistically significant (P = 0.621; Figure 4). Meanwhile, the thickness of capsules to BellaGel SmoothFine® (680.58 ± 46.64 μm) and Motiva SilkSurface® (775.92 ± 49.66 μm) were significantly thinner than those surrounding the BellaGel Smooth® ($P < 0.05$) and BellaGel Textured® surfaces ($P < 0.05$). These results clearly indicate a close relationship between implant texture and the capsule thickness.

3.4. Effect of BellaGel SmoothFine® Implant on Collagen Density

To evaluate the collagen density, the sections were subjected to MT staining, there was a significantly greater increased collagen density to both BellaGel Smooth® (62.3% ± 1.18%) and BellaGel Textured® (61.01% ± 0.61%) surface (Figure 5). There were no significant differences in collagen density between the BellaGel Smooth® and the BellaGel Textured® group ($P > 0.05$; Figure 5). In contrast, a significant reduction in the rate of MT-positive tissue was seen both in the BellaGel SmoothFine® (54.2% ± 3.5%; $P = 0.042$) and Motiva SilkSurface® (55.3% ± 2.12%; $P = 0.011$) related to the BellaGel Smooth® (Figure 5).

3.5. Effect of BellaGel SmoothFine® Implant on iNOS and Arg-1 Expression

iNOS levels are crucial to quantify local inflammatory response. As seen in Figure 6, at the 1-week point, the levels of iNOS around the BellaGel Smooth® and BellaGel Textured® surface appeared significantly overexpressed than those around the BellaGel SmoothFine® and Motiva SilkSurface® (Figure 6). The mean relative expression level was 1.27 ± 0.18 in the BellaGel Smooth® group, compared with 0.81 ± 0.11 in the BellaGel Textured® group (Figure 6). This difference was not

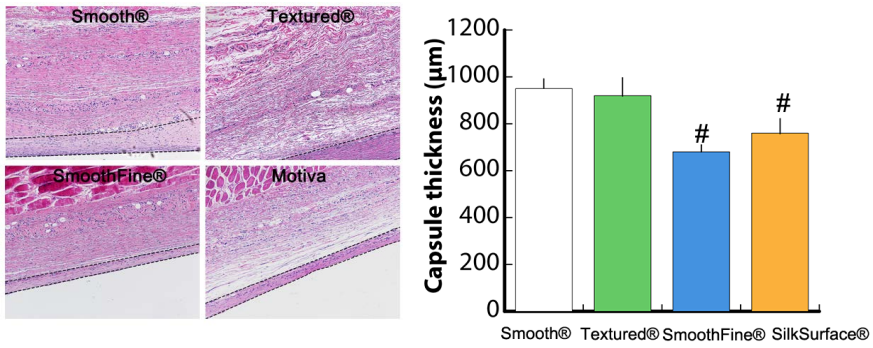

(a) (b)

Figure 4. The effect of BellaGel SmoothFine® implant on capsule formation. (a) Capsule tissues at the tissue-implant interface at 8 weeks were stained with hematoxylin and eosin (H & E). (b) The capsule thickness was measured. Five randomly selected tissue sections per rat were counted. Data are represented as the mean ± S.E.M. with n = 5 rats per group. #$P < 0.05$, significantly different from BellaGel Smooth implant. Original magnification ×400, scale bar = 100 μm.

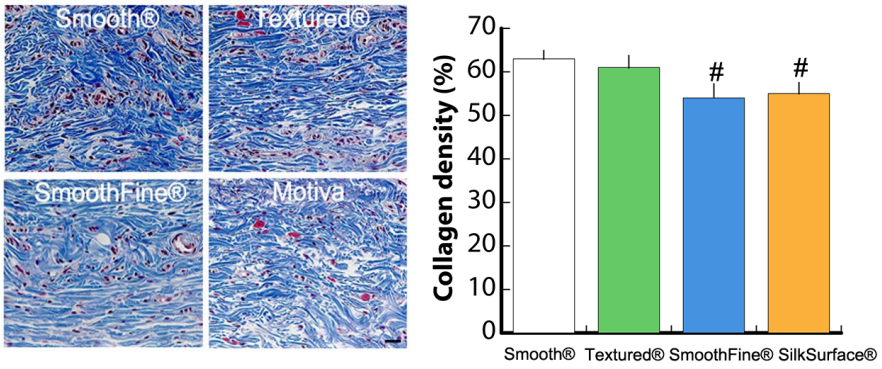

Figure 5. The effect of BellaGel SmoothFine® implant on collagen density. (a) Capsule tissues at the tissue-implant interface at 8 weeks were stained with Masson's Trichrome (MT). (b) The collagen density was measured. Five randomly selected tissue sections per rat were counted. Data are represented as the mean ± S.E.M. with n = 5 rats per group. #$P <$ 0.05, significantly different from BellaGel Smooth implant (independent *t*-test). Original magnification ×400, scale bar = 100 μm.

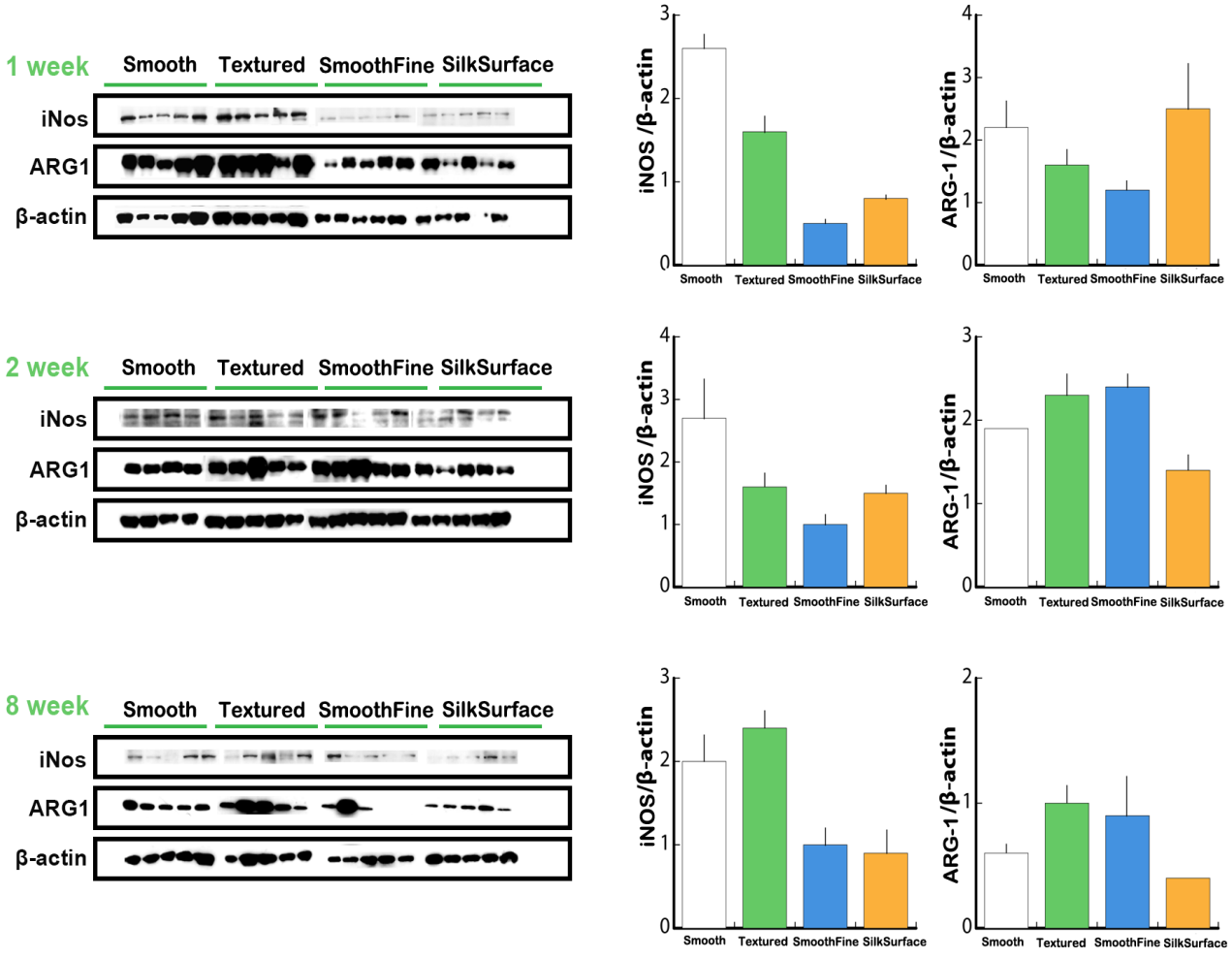

Figure 6. The effect of BellaGel SmoothFine® implant on iNOS and Arg-1 expression. Silicone breast implants were emplaced beneath the panniculus carnosus muscle on the dorsum of Sprague Dawley rats and the fibrous capsule tissues at the tissue-implant interface at 1 week, 2 weeks, 8 weeks were extracted explanted for histological examination. Expressions of iNOS and Arg-1 were detected by immunoblot analysis. Data are represented as the mean ± S.E.M. with n = 5 rats per group.

statistically significant ($P = 0.072$; Figure 6). Meanwhile, the relative expression level to BellaGel SmoothFine® (0.24 ± 0.03) and Motiva SilkSurface® (0.38 ± 0.04) were significantly lower than those surrounding the BellaGel Smooth® ($P < 0.05$) and BellaGel Textured® surfaces ($P < 0.05$). This result provides evidence of a more severe inflammatory reaction against BellaGel Smooth® than against BellaGel SmoothFine® or Motiva SilkSurface®. At the 2-week point, iNOS levels also tended to decrease when compared with the BellaGel Smooth® and BellaGel Textured®, although this decrease was not significant (Figure 6). In contrast, at 8 weeks, the level of iNOS expression peaked in the BellaGel Textured® surface (mean = 1.22). The BellaGel SmoothFine® surface (mean = 0.55) and Motiva SilkSurfaces® (mean = 0.54) showed a significantly lower level of iNOS than the BellaGel Smooth® surface (mean = 1.02) (Figure 6). However, Arg-1 expression was not affected significantly ($P > 0.05$). In all groups analyzed (1, 2, and 8 weeks), the expression of iNOS was higher in the BellaGel Smooth® and the BellGel Textured® surfaces, it was statistically significant than BellaGel SmoothFine® and Motiva SilkSurfaces®.

3.6. Effect of BellaGel SmoothFine® Implant on Vimentin and α-SMA Expression

Vimentin and SMA are molecular markers of fibrosis. After 1 week, there was a greater increased Vimentin expression to both BellaGel Smooth® and BellaGel Textured® surfaces in comparison to both BellaGel SmoothFine® (BellaGel Smooth® $P = 0.12$; BellaGel Textured® $P = 0.042$) and Motiva SilkSurface® (BellaGel Smooth® $P = 0.12$; BellaGel Textured® $P = 0.044$) (Figure 7). At the 2-week point, Vimentin levels to BellaGel SmoothFine® also tended to decrease when compared with the BellaGel Smooth®, although this decrease was not significant ($P = 0.449$; Figure 7). At the 2-week point, we did not observe any difference between them. In contrast, at 8 weeks, the Motiva SilkSurface® group showed a significantly lower level of Vimentin than the BellaGel Smooth® ($P = 0.015$; Figure 7). However, there was no significant differences in the BellaGel Smooth® in comparison to BellaGel SmoothFine® ($P = 0.377$). There was a significant increase in myofibrobalsts in the capsule around the BellaGel Smooth® surfaces. Notably, formation of α-SMA-negative stress fibers was also reduced on the Motiva SilkSurface® was completely absent from 1 week to 8 weeks (Figure 7).

4. Discussion

The BellaGel SmoothFine® implant is a novel nanotextured breast implant. On a clinical level, BellaGel SmoothFine® demonstrated excellent safety outcomes and reduced serious adverse events such as double capsules, capsular contracture, implant rupture for device failure, or late seromas [23]. In the current study, we investigated the physical properties of BellaGel SmoothFine® surfaces and the effect and underlying mechanisms of BellaGel SmoothFine® on the capsular contracture *in vivo* animal model.

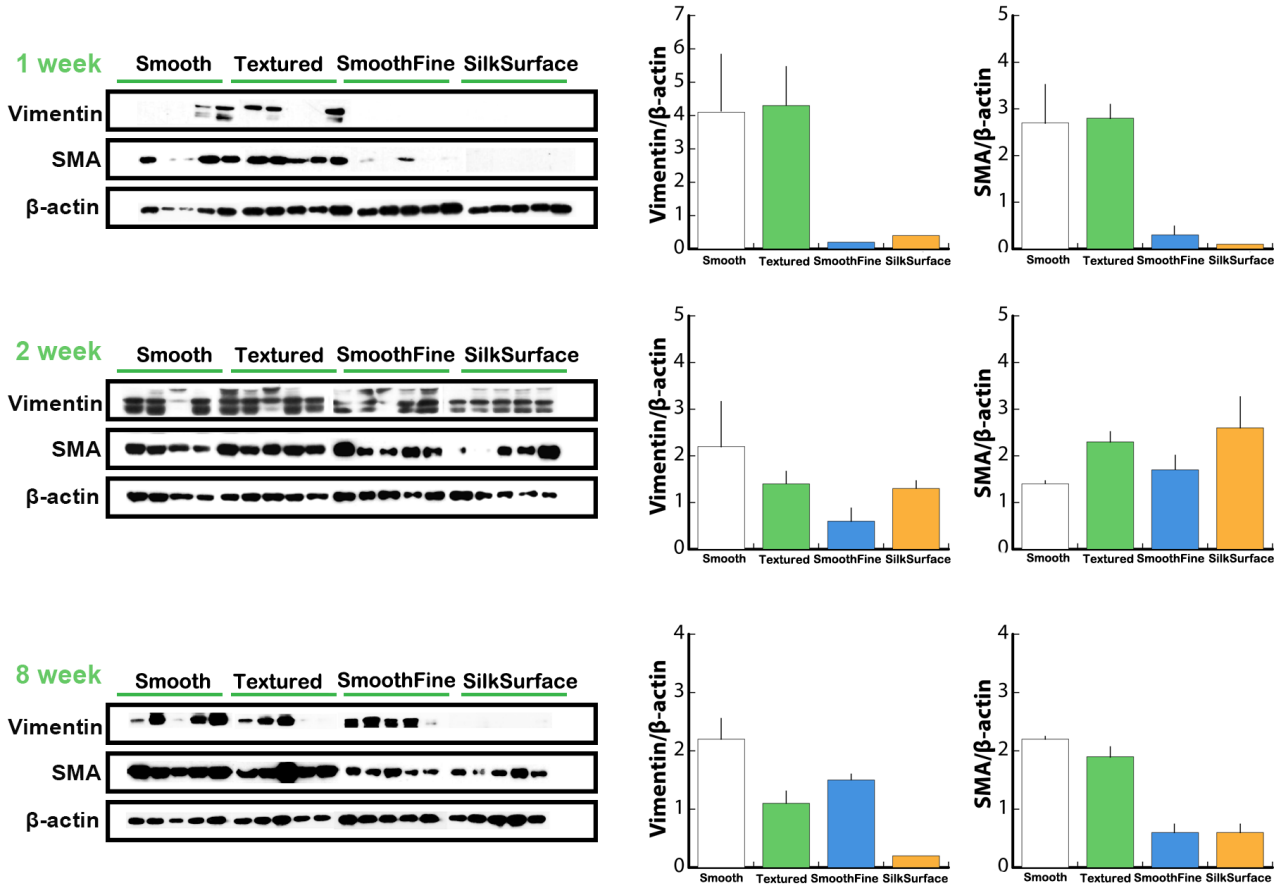

Figure 7. The effect of BellaGel SmoothFine® implant on Vimentin and *α*-SMA expression. Silicone breast implants were emplaced beneath the panniculus carnosus muscle on the dorsum of Sprague Dawley rats and the fibrous capsule tissues at the tissue-implant interface at 1 week, 2 weeks, 8 weeks were extracted explanted for histological examination. Expressions of Vimentin and *α*-SMA were detected by immunoblot analysis. Data are represented as the mean ± S.E.M. with n = 5 rats per group.

BellaGel SmoothFine® has a low surface roughness value at a subcellular level, which implies less particle friction coefficients and no tissue ingrowth [24] [25]. A skewness value of 0.36 ± 0.19, a kurtosis value of 4.23 ± 0.68 and a contact angle of 103.14˚ ± 2.06˚, are known to show higher biocompatibility. Therefore, we expected that BellaGel SmoothFine® may have led to the blocking of fibrous capsule formation in the current study.

Collagenous capsules formation is an inevitable response to all kind of foreign bodies and is always occur after silicone breast implant insertion into the body. Externally, a capsule develops a relatively undetectable thin membrane surrounding the implant in those undergoing breast augmentations. However, a stronger foreign body reaction to the implant leads to more excessive hypocellular thicker capsule formation, which is rich in collagen and positively related to the contracture formation [26]. This can cause an abnormally hard feel of the implant and pain in the breast. Previous study reported that surface texture may predispose implants to excessive capsular formation [9] [27]. Smooth surfaces are known to be correlated with high prevalence of capsular contracture, because fibroblasts on the surface of smooth textured implant produce collagen fibers,

which are align highly within the capsule next to the implant in response to a shearing motion within the implant pocket [28] [29]. The continual rubbing between a smooth-surfaced implant and its nonadherent capsule plays a key role in causing a thick capsule and an acute, active tissue response [30]. By contrast, textured surfaces disrupt certain collagen alignment of the surrounding capsule through inhibiting micromotion at the porsthesis/host interface. Therefore, textured surfaces induce decreased malposition and capsular contracture with respect to smooth surfaces [5] [8] [12] [28] [31] [32] [33]. However, additional studies showed no statistically significant reduction in the capsule formation [33]-[39]. In the present study, we conducted an experiment in which silicone implants were emplaced beneath the muscle layer in rat, and the capsules that developed surrounding the silicone implants were then investigated. BellaGel SmoothFine® surfaces promoted significantly decreased collagenous capsule thickness in comparison to the BellaGel Smooth® and BellaGel Textured® surfaces. In addition, the collagen densities in the capsules surrounding the BellaGel SmoothFine® and Motiva SilkSurfaces® were significantly decreased with respect to the BellaGel Smooth® and BellaGel Textured®. The hierarchical nano-texutred surfaces of the BellaGel SmoothFine® implant, together with its perceived roughness may lead to the dramatic reduction of capsule thickness and collagen density as well.

Inflammatory reaction occurred when silicone breast implant inserted into the body, plays a vital role in the progression of capsular contracture, because it activates fibroblasts around capsules to cause excessive fibrosis and hypertrophic scar contracture [40] [41]. iNOS, a degradative enzyme, is an acute phase inflammatory factor and expressed by macrophages. They seem central to degrade the silicone breast implant through the production of nitric oxide. Significantly, iNOS is important in the pathogenesis of breast implant derived capsular contracture [42] [43]. In this work we found that the expression of iNOS was reduced on BellaGel SmoothFine® and Motiva SilkSurfaces® in comparison to BellaGel Smooth® and Textured® surfaces. The constant rubbing between a smooth surfaces implant and host tissue might induce significantly increased inflammatory response [30]. The reduction in frictional forces between the textured surfaces and host tissues may result in minimal inflammation with respect to smooth surfaces. However, frequent cracking of the collagen fibers on textured surfaces may cause persistent inflammation. BellaGel SmoothFine® is not rough enough to cause friction with the surrounding tissues; therefore, the initial inflammatory response was decreased.

Fibroblasts differentiate into myofibroblasts in contracted fibrous capsules and upregulate the expression of IL-8, TGF-β, TGF-β 1, α-SMA, collagen 1, and MMP12 as they differentiate into capsular myofibroblasts [21]. Myofibroblasts present in some conditions associated with contraction processes, such as tenosynovitis, Dupuytren's contracture, and fibrous capsules formed around implant [44]. Inside the body, fibroblasts and myofibroblasts are known to make a stiff extracellular matrix that remodels the original healthy tissue. An abundance of

vimentin positive fibroblasts and α-SMA positive myofibroblasts were seen in contracted capsules, and were relatively absent in normal breast tissue. Our result showed that the BellaGel SmoothFine® induced decreased expression of Vimentin and α-SMA in comparion to BellaGel Smooth® and BellaGel Textured®. This results indicated that silicone breast implant with nano texture inhibited BI-induced capsular contracture by inhibiting the proliferation of fibroblast and myofibroblasts.

In conclusion, our study showed that variations in surface roughness of breast implant influenced breast implant derived fibrous capsule formation. Of note, surface texture with nano-textured implant such as BellaGel SmoothFine® and Motiva SilkSurfaces® can affect the pathophysiology of the foreign body reaction, causing less capsule formation, inflammation, and influx of fibroblasts, which contributes to the development of capsular contracture.

Acknowledgements

The study was supported by grant No. 02-2013-121 from SNUBH Research Fund, and a grant from the Korea Health Technology R&D Project through the Korea Health Industry Development Institute (KHIDI), funded by the Ministry of Health & Welfare, Republic of Korea (grant number: HI15C1744).

Conflicts of Interest

The authors declare no conflicts of interest regarding the publication of this paper.

References

[1] Anderson, J.M., Rodriguez, A. and Chang, D.T. (2008) Foreign Body Reaction to Biomaterials. *Seminars in Immunology*, **20**, 86-100. https://doi.org/10.1016/j.smim.2007.11.004

[2] American Society of Plastic Surgeons (2013) Plastic Surgery Statistics Report.

[3] Araco, A., Caruso, R., Araco, F., Overton, J. and Gravant, G. (2009) Capsular Contractures: A Systematic Review. *Plastic Reconstructive Surgery*, **124**, 1808-1819. https://doi.org/10.1097/PRS.0b013e3181bf7f26

[4] Handel, N., Cordray, T., Gutierrez, J., *et al*. (2006) A Long-Term Study of Outcomes, Complications, and Patient Satisfaction with Breast Implants. *Plastic Reconstructive Surgery*, **117**, 757-767. https://doi.org/10.1097/01.prs.0000201457.00772.1d

[5] Headon, H., Kasem, A. and Mokbel, K. (2015) Capsular Contracture after Breast Augmentation: An Update for Clinical Practice. *Archives of Plastic Surgery*, **42**, 532-543. https://doi.org/10.5999/aps.2015.42.5.532

[6] Rosato, R.M. and Dowden, R.V. (1994) Radiation-Therapy as a Cause of Capsular Contracture. *Annals of Plastic Surgery*, **32**, 342-345. https://doi.org/10.1097/00000637-199404000-00002

[7] Cash, T.F., Duel, L.A. and Perkins, L.L. (2002) Women's Psychosocial Outcomes of Breast Augmentation with Silicone Gel-Filled Implants: A 2-Year Prospective Study. *Plastic and Reconstructive Surgery*, **109**, 2112-2121. https://doi.org/10.1097/00006534-200205000-00049

[8] Harvey, A.G., Hill, E.W. and Bayat, A. (2013) Designing Implant Surface Topography for Improved Biocompatibility. *Expert Review of Medical Devices*, **10**, 257-267. https://doi.org/10.1586/erd.12.82

[9] Barr, S. and Bayat, A. (2011) Breast Implant Surface Development: Perspectives on Development and Manufacture. *Aesthetic Surgery Journal*, **31**, 56-67. https://doi.org/10.1177/1090820X10390921

[10] Barr, S., Hill, E. and Bayat, A. (2009) Current Implant Surface Technology: An Examination of Their Nanostructure and Their Influence on Fibroblast Alignment and Biocompatibility. *Eplasty*, **9**, e22.

[11] Valencia-Lazcano, A.A., Alonso-Rasgado, T. and Bayat, A. (2013) Characterisation of Breast Implant Surfaces and Correlation with Fibroblast Adhesion. *Journal of the Mechanical Behavior of Biomedical Materials*, **21**, 133-148. https://doi.org/10.1016/j.jmbbm.2013.02.005

[12] Barnsley, G.P., Sigurdson, L.J. and Barnsley, S.E. (2006) Textured Surface Breast Implants in the Prevention of Capsular Contracture among Breast Augmentation Patients: A Meta-Analysis of Randomized Controlled Trials. *Plastic and Reconstructive Surgery*, **117**, 2182-2190. https://doi.org/10.1097/01.prs.0000218184.47372.d5

[13] Wong, C.H., Samuel, M., Tan, B.K., *et al*. (2006) Capsular Contracture in Subglandular Breast Augmentation with Textured versus Smooth Breast Implants: A Systematic Review. *Plastic and Reconstructive Surgery*, **118**, 1224-1236. https://doi.org/10.1097/01.prs.0000237013.50283.d2

[14] Hall-Findlay, E.J. (2011) Breast Implant Complication Review: Double Capsules and Late Seromas. *Plastic and Reconstructive Surgery*, **127**, 56-66. https://doi.org/10.1097/PRS.0b013e3181fad34d

[15] Doren, E.L., Miranda, R.N., Selber, J.C., *et al*. (2017) U.S. Epidemiology of Breast Implant-Associated Anaplastic Large Cell Lymphoma. *Plastic and Reconstructive Surgery*, **139**, 1042-1050. https://doi.org/10.1097/PRS.0000000000003282

[16] Anselme, K. and Bigerelle, M. (2011) Role of Materials Surface Topography on Mammalian Cell Response. *International Materials Reviews*, **56**, 243-266. https://doi.org/10.1179/1743280411Y.0000000001

[17] Flemming, R.G., Murphy, C.J., Abrams, G.A., *et al*. (1999) Effects of Synthetic Micro- and Nano-Structured Surfaces on Cell Behavior. *Biomaterials*, **20**, 573-588. https://doi.org/10.1016/S0142-9612(98)00209-9

[18] Hajicharalambous, C.S., Lichter, J., Hix, W.T., *et al*. (2009) Nano- and Sub-Micron Porous Polyelectrolyte Multilayer Assemblies: Biomimetic Surfaces for Human Corneal Epithelial Cells. *Biomaterials*, **30**, 4029-4036. https://doi.org/10.1016/j.biomaterials.2009.03.020

[19] Kulangara, K., Adler, A.F., Wang, H., *et al*. (2014) The Effect of Substrate Topography on Direct Reprogramming of Fibroblasts to Induced Neurons. *Biomaterials*, **35**, 5327-5336. https://doi.org/10.1016/j.biomaterials.2014.03.034

[20] Nikkhah, M., Edalat, F., Manoucheri, S., *et al*. (2012) Engineering Microscale Topographies to Control the Cell-Substrate Interface. *Biomaterials*, **33**, 5230-5246. https://doi.org/10.1016/j.biomaterials.2012.03.079

[21] Kyle, D.J., Oikonomou, A., Hill, E., *et al*. (2015) Development and Functional Evaluation of Biomimetic Silicone Surfaces with Hierarchical Micro/Nano-Topographical Features Demonstrates Favourable *in Vitro* Foreign Body Response of Breast-Derived Fibroblasts. *Biomaterials*, **52**, 88-102. https://doi.org/10.1016/j.biomaterials.2015.02.003

[22] Langer, R. and Tirrell, D.A. (2004) Designing Materials for Biology and Medicine. *Nature*, **428**, 487-492. https://doi.org/10.1038/nature02388

[23] Han, J., Jeong, J.H. and Bang, S.H. (2019) BellaGel Breast Implant: 4-Year Results of a Prospective Cohort Study. *Journal of Plastic Surgery and Hand Surgery*, **53**, 232-239. https://doi.org/10.1080/2000656X.2019.1583572

[24] Barr, S., Hill, E.W. and Bayat, A. (2017) Functional Biocompatibility Testing of Silicone Breast Implants and a Novel Classification System Based on Surface Roughness. *Journal of the Mechanical Behavior of Biomedical Materials*, **75**, 75-81. https://doi.org/10.1016/j.jmbbm.2017.06.030

[25] Munhoz, A.M., di Pompeo, F.S. and De Mezerville, R. (2017) Nanotechnology, Nanosurfaces and Silicone Gel Breast Implants: Current Aspects. *Case Reports in Plastic Surgery and Hand Surgery*, **4**, 99-113. https://doi.org/10.1080/23320885.2017.1407658

[26] Vieira, V.J., d'Acampora, A.J., Marcos, A.B.W., *et al*. (2010) Vascular Endothelial Growth Factor Overexpression Positively Modulates the Characteristics of Periprosthetic Tissue of Polyurethane-Coated Silicone Breast Implant in Rats. *Plastic Reconstructive Surgery*, **126**, 1899-1910. https://doi.org/10.1097/PRS.0b013e3181f446d5

[27] Berry, M.G. and Davies, D.M. (2010) Breast Augmentation: Part I—A Review of the Silicone Prosthesis. *Journal of Plastic, Reconstructive & Aesthetic Surgery*, **63**, 1761-1768. https://doi.org/10.1016/j.bjps.2009.07.047

[28] Brohim, R.M., Foresman, P.A., Hildebrandt, P.K., *et al*. (1992) Early Tissue Reaction to Textured Breast Implant Surfaces. *Annals of Plastic Surgery*, **28**, 354-362. https://doi.org/10.1097/00000637-199204000-00010

[29] Danino, M.A., Efanov, J.I., Dimitropoulos, G., *et al*. (2018) Capsular Biofilm Formation at the Interface of Textured Expanders and Human Acellular Dermal Matrix: A Comparative Scanning Electron Microscopy Study. *Plastic Reconstructive Surgery*, **141**, 919-928. https://doi.org/10.1097/PRS.0000000000004216

[30] Snow, J., Harasaki, H., Kasick, J., *et al*. (1981) Promising Results with a New Textured Surface Intrathoracic Variable Volume Device for LVAS. *Transactions—ASAIO American Society for Artificial Internal Organs*, **27**, 485-489.

[31] Clugston, P.A., Perry, L.C., Hammond, D.C. and Maxwell, G.P. (1994) A Rat Model for Capsular Contracture: The Effects of Surface Texturing. *Annals of Plastic Surgery*, **33**, 595-599. https://doi.org/10.1097/00000637-199412000-00005

[32] Derby, B.M. and Codner, M.A. (2015) Textured Silicone Breast Implant Use in Primary Augmentation: Core Data Update and Review. *Plastic Reconstructive Surgery*, **135**, 113-124. https://doi.org/10.1097/PRS.0000000000000832

[33] Hakelius, L. and Ohlsen, L. (1997) Tendency to Capsular Contracture around Smooth and Textured Gel-Filled Silicone Mammary Implants: A 5-Year Follow-Up. *Plastic Reconstructive Surgery*, **100**, 1566-1569. https://doi.org/10.1097/00006534-199711000-00030

[34] Coleman, D.J., Sharpe, D.T., Naylor, I.L., *et al*. (1993) The Role of the Contractile Fibroblast in the Capsules around Tissue Expanders and Implants. *British Journal of Plastic Surgery*, **46**, 547-556. https://doi.org/10.1016/0007-1226(93)90104-J

[35] Malata, C.M., Feldberg, L., Coleman, D.J., *et al*. (1997) Textured or Smooth Implants for Breast Augmentation? Three Year Follow-Up of a Prospective Randomised Controlled Trial. *British Journal of Plastic Surgery*, **50**, 99-105. https://doi.org/10.1016/S0007-1226(97)91320-5

[36] Collis, N., Coleman, D., Foo, I.T.H., *et al*. (2000) Ten-Year Review of a Prospective

Randomized Controlled Trial of Textured versus Smooth Subglandular Silicone Gel Breast Implants. *Plastic Reconstructive Surgery*, **106**, 786-791. https://doi.org/10.1097/00006534-200009020-00005

[37] Burkhardt, B.R. and Demas, C.P. (1994) The Effect of Siltex Texturing and Povidone-Iodine Irrigation on Capsular Contracture around Saline Inflatable Breast Implants. *Plastic Reconstructive Surgery*, **93**, 123-128. https://doi.org/10.1097/00006534-199401000-00018

[38] Burkhardt, B.R. and Eades, E. (1995) The Effect of Biocell Texturing and Povidone-Iodine Irrigation on Capsular Contracture around Saline-Inflatable Breast Implants. *Plastic Reconstructive Surgery*, **96**, 1317-1325. https://doi.org/10.1097/00006534-199511000-00013

[39] Fagrell, D., Berggren, A. and Tarpila, E. (2001) Capsular Contracture around Saline-Filled Fine Textured and Smooth Mammary Implants: A Prospective 7.5-Year Follow-Up. *Plastic Reconstructive Surgery*, **108**, 2108-2112. https://doi.org/10.1097/00006534-200112000-00047

[40] Ibrahim, M.M., Bond, J., Bergeron, A., *et al*. (2014) A Novel Immune Competent Murine Hypertrophic Scar Contracture Model: A Tool to Elucidate Disease Mechanism and Develop New Therapies. *Wound Repair and Regeneration*, **22**, 755-764. https://doi.org/10.1111/wrr.12238

[41] Orciani, M., Lazzarini, R., Scartozzi, M., *et al*. (2013) The Response of Breast Cancer Cells to Mesenchymal Stem Cells: A Possible Role of Inflammation by Breast Implants. *Plastic Reconstructive Surgery*, **132**, 899e-910e. https://doi.org/10.1097/01.prs.0000434401.98939.60

[42] Leung, T.M., Fung, M.L., Liong, E.C., *et al*. (2011) Role of Nitric Oxide in the Regulation of Fibrogenic Factors in Experimental Liver Fibrosis in Mice. *Histology and Histopathology*, **26**, 201-211.

[43] Fielding, C.A., Jones, G.W., McLoughlin, R.M., *et al*. (2014) Interleukin-6 Signaling Drives Fibrosis in Unresolved Inflammation. *Immunity*, **40**, 40-50. https://doi.org/10.1016/j.immuni.2013.10.022

[44] Rudoph, R., Guber, S., Suzaki, M., *et al*. (1977) The Life Cycle of the Myofibroblast. *Surgery, Gynecology & Obstetrics*, **145**, 389.